10 Synthesis, characterization and computational studies of 1,3-bis[(E)-furan-2-yl)methylene]urea and 1,3-bis[(E)-furan-2-yl)methylene]thiourea

Chapter · June 2021

DOI: 10.1515/9783110682045-010

CITATION
1

READS
123

5 authors, including:

Kazeem Adelani Alabi
Fountain University Osogbo Nigeria
45 PUBLICATIONS **240** CITATIONS
SEE PROFILE

Ibrahim Abdulsalami
Fountain University Osogbo Nigeria
25 PUBLICATIONS **133** CITATIONS
SEE PROFILE

Moriam Dasola Adeoye
Fountain University Osogbo Nigeria
55 PUBLICATIONS **250** CITATIONS
SEE PROFILE

Shukurat Aderinto
Fountain University Osogbo Nigeria
4 PUBLICATIONS **2** CITATIONS
SEE PROFILE

Kazeem Adelani Alabi*, Ibrahim Olasegun Abdulsalami, Moriam Dasola Adeoye, Shukurat Modupe Aderinto and Rasheed Adewale Adigun

Synthesis, characterization and computational studies of 1,3-bis[(*E*)-furan-2-yl)methylene]urea and 1,3-bis[(*E*)-furan-2-yl) methylene]thiourea

Abstract: Urea and thiourea derivatives: 1,3-bis[**(*E*)-**furan-2-yl)methylene]urea (BFMU) and 1,3-bis[**(*E*)-**furan-2-yl)methylene]thiourea (BFMT) were synthesized and characterized by spectrometry analyses (UV, IR, ^{1}H NMR and ^{13}C NMR). They were screened for antibacterial (*Salmonella typhi, Staphylococcus aureus, Pseudomonas aeruginosa, Xanthomonas axonopodis* and *Streptococcus bovis*) and antifungal (*Fusarium oxysporum*, *Colletotrichum gloeosporioides and Cercospora zeae-maydis*) activities. Quantum chemical calculations of frontier molecular orbital energies (E_{HOMO} and E_{LUMO}), and their associated global parameters were carried out by DFT levels of theory, with complete relaxation in the potential energy surface using 6-31G* basis set (DFT/B3LYP/6-31G*). Azomethine functional groups (C=N) appeared at δ 7.6 ppm and δ 7.0 ppm in the proton spectra, the peaks between δ 105 and δ 160 ppm of ^{13}C spectra represent the methylene carbons (C=C). BFMU is a better inhibitor of *P. aeruginosa* and *S. bovis*, while BFMT is a better inhibitor of *S. typhi*, *S. aureus* and *X. axonopodis* and the fungi isolates (*F. oxysporum*, *C. gloeosporioides* and *C. zeae-maydis*) used. The global parameters agreed favorably with the experimental results, indicating the higher activity of BFMT.

Keywords: 1,3-bis[**(*E*)-**furan-2-yl)methylene]thiourea, 1,3-bis[**(*E*)-**furan-2-yl)methylene]urea, furfural and NMR spectra

***Corresponding author: Kazeem Adelani Alabi**, Ph.D, Department of Chemical Sciences, Organic Synthesis and Natural Product Group, Fountain University, Osogbo, Nigeria.
E-mail: qasimade@gmail.com
Ibrahim Olasegun Abdulsalami and Moriam Dasola Adeoye, Department of Chemical Sciences, Theoretical and Computational Chemistry Group, Fountain University, Osogbo, Nigeria,
E-mail: aiboldkip@gmail.com (I.O. Abdulsalami), dasoladeoye@yahoo.com (M.D. Adeoye)
Shukurat Modupe Aderinto, Department of Chemical Sciences, Industrial and Environmental Chemistry Unit, Fountain University, Osogbo, Nigeria, E-mail: modupe4995@gmail.com
Rasheed Adewale Adigun, Department of Chemistry, University of Pretoria, Pretoria, South Africa,
E-mail: activatedrasheed@gmail.com

https://doi.org/10.1515/psr-2019-0134

1 Introduction

Furfural is renewable with numerous industrial uses; it could be used as a solvent and starting material for the production of various agrochemicals, pharmaceuticals and fragrances [1, 2]. Mostly, concentrated tetraoxosulphate (vi) acid is used for the extraction of furfural [3].

In order to further look into the furfural's industrial uses, researchers now synthesize furfural from different sources; they could transform pentose into furfural using a heterogeneous catalyst, which is both economical and environmental friendly [4]. Hybrid inorganic–organic solid acid catalysts are recently used to achieve better dehydration of xylose. For instance, Moreu et al. [5] discovered that microporous zeolites (mordenites and faujasites) could be used as catalysts in the production of furfural from xylose [6, 8]. Zeolite Nu—6(1) has also been used to dehydrate xylose [7].

Furfuryl alcohol is a useful chemical intermediate for the production of furan resin prepolymeric material which in turn is used in the production of thermoset polymer, cements, adhesives, resin and coating materials.

Hydrogenation of furfural alcohol also leads to the production of tetrahydrofurfuryl alcohol (THFA) which is used as a nonhazardous solvent especially in agriculture. Furfural is converted into furoic acid by oxidation reaction and into furan by decarboxylation with the help of palladium as a catalyst [4]. It has many other applications as antacids, fertilizers, inks, antifungi and antinematodes, while its by-product is a useful flavoring agent [9, 10]. Resins produced from furfuryl acid have also been reported to have excellent thermal, physicochemical properties and are also inert to solvents.

Bis-imines are biologically active because of azomethine (>C=N) functional group [11]. They form useful complexes with metallic ions through azomethine and phenolic functional groups [12]. Azomethines, prepared from primary amines and aldehydes, are useful substrates to prepare many useful compounds through different methods. Some of the biological activities are as antimicrobial, fungicidal, antitumor and herbicidal agents. Azomethines are good ligands for complexation of metal ions yielding compounds of enhanced physicochemical and biological properties [13]. Moreover, there are enough information on the reactions and physicochemical properties of five-membered rings with azomethine functional group, but the bi-cyclic and macrocyclic azomethines have not been thoroughly investigated. Thus, they have now received much attention in chemistry and biology [14].

In an attempt to contribute to this growing area of research, this study focused on characterization of the synthesized furfural derivatives with azomethines moieties (BFMU and BFMT), using proton and ^{13}C NMR. These synthesized compounds were screened for their potential antibacterial and antifungal activities.

The frontier molecular orbital characteristics and their associated properties (such as: dipole moment [μ], polarizabilities [α], electronegativity/chemical potential [χ], global chemical hardness [η], nucleophilicity and electrophilicity indices [ω]) which

play significant roles in the prediction of the stabilities and efficiency of molecules were also theoretically determined for the compounds.

2 Materials and methodologies

2.1 Experimental details

2.1.1 Chemical and apparatus: Fulfural, urea, thiourea, ethanol/methanol, acetone, chloroform and glacial acetic acid were bought from British Drug House Chemical Ltd. (BDH) and MRS Scientific Ltd. Furfural was purified by distillation, and kept in an amber bottle to avoid atmospheric auto-oxidation, before use.

2.1.2 Synthesis of 1,3-bis[(*E*)-furan-2-yl)methylene]urea: Redistilled furfural (10 g) was dissolved in ethanol (5 mL) mixed with urea (6.25 g). Two to three (2–3) drops of glacial acetic acid were added to the mixture, which was refluxed for 60 min. The reaction mixture was then poured on to 250 mL cold water when cooled. The product was filtered, washed with water and recrystallized in alcohol [11] (see Scheme 1).

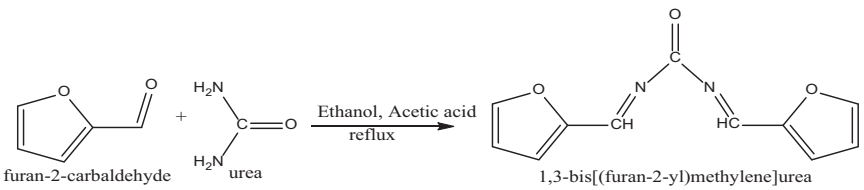

Scheme 1: Synthesis of 1,3-bis[(*E*)-furan-2-yl)methylene]urea.

2.1.3 Synthesis of 1,3-bis[(*E*)-furan-2-yl)methylene]thiourea: Redistilled furfural (10 g) was dissolved in ethanol (5 mL) in the presence of thiourea (7.90 g). Two-three drops of glacial acetic acid were added and the mixture refluxed for 90 min. On cooling, the reaction mixture was poured on to 250 mL cold water. The product was filtered, washed with water and recrystallized in alcohol [11] (see Scheme 2).

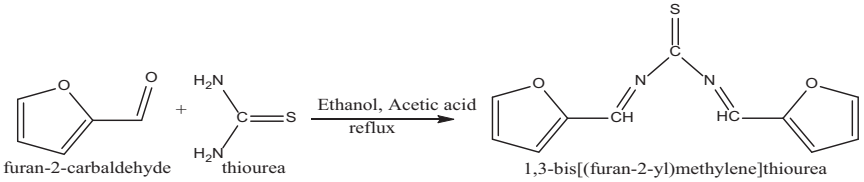

Scheme 2: Synthesis of 1,3-bis[(*E*)-furan-2-yl)methylene]thiourea.

2.1.4 Determination of melting point of the products: Capillary melting points method was used for the determination of the melting point of the products.

2.1.5 Ultraviolet visible analysis: The UV/visible spectroscopy was determined in acetic acid and acetone at room temperature using 6405 UV/visible Spectrophotometer in the region 200–800 nm.

2.1.6 Infrared spectroscopy analysis: This was determined on a Shimadu Fourier Transformed Infrared Spectrophotometer (FT-IR) between 500 and 4000 cm^{-1} with KBr disc [15].

2.1.7 Nuclear magnetic resonance (NMR) analysis: ^{1}H NMR and ^{13}C NMR spectra were obtained with Agilent-NMR-vnmrs 400 with pulse sequence: proton (s2pul), temperature 26.0 °C/ 299.1 K, relaxation delay 1.000 s, pulse 45.0°, aqueous time 2.556 s, and width 6410.3 Hz spectrometer using deuterated dimethylsulfoxide (DMSO) as solvent [16].

2.1.8 Antibacteria activities of the compounds: *Salmonella typhi, Staphylococcus aureus, Pseudomonas aeruginosa, Xanthomonas axonopodis* and *Streptococcus bovis* were cultured aerobically at 37 °C for a day on peptone water and antimicrobial testing were carried out on the nutrient agar plates. The fungi were also grown aerobically at 27 °C on potato Dextrose agar (P.D.A) plates. Agar well diffusion methods described by Norrel and Messely were used with little modification. Pure isolate of each bacterium was cultured in peptone water for one and half to two days.

These were seeded on the sterile nutrient agar (NA) plate containing 8 mm wells. Each sample 0.5 mL of (0.02 g/mL) concentration was introduced into the bore agar well and incubated for 24 h at 37 °C. Control plates was also set up using dimethylformamide (DMF), methanol and standard antibiotics Streptomycine sulfate and tetracycline at 0.02 g/mL and incubated as above. Zones of inhibition were measured and recorded in mm.

2.1.9 Antifungal activities of the compounds: The fungi of choice were: *Fusarium oxysporum Colletotrichum gloeosporioides* and *Cercospora zeae-maydis*. Samples (0.02 g/mL) were prepared and 0.5 mL of each samples were aseptically mixed with 15 mL of sterile molten potato dextrose agar (P.D.A.). The fungi were inoculated at the center of the plate with the aid of 4 mm cork borer, sterile needle and syringe. Benlate, a standard antifungal agent was used as a control. Dimethylformamide (D.M.F.) and methanol impregnated plates were equally prepared. All the plates were incubated at 27 °C for 72 h while mycelia growth was measured at 24 h interval. After 72 h, mycelia growth inhibition was measured and calculated in percentage.

2.2 Computational results

Using the molecular editor builder of SPARTAN 09 [15], BFMU ($C_{11}H_8N_2O_3$) and BFMT ($C_{11}H_8N_2O_2S$) were modeled and minimized. The minimized structures of the molecules were run using SPARTAN 09 software with molecular orbital calculation at DFT/B3LYP/6-31G* level of theory in vacuum. The optimized geometries of the studied molecules (Figure 1) were then used to obtain the ground state molecular geometry parameters: dipole moment, polarizabilities, the frontier molecular orbital energies of the studied molecules at the same level of theory [17]. The E_{HOMO}/E_{LUMO} energy gaps and associated qualitative structure activity relationship (QSAR) properties, i.e. chemical potential, ionization energy, global softness and global hardness (η), electrophilicity index and nucleophilicity index were also calculated.

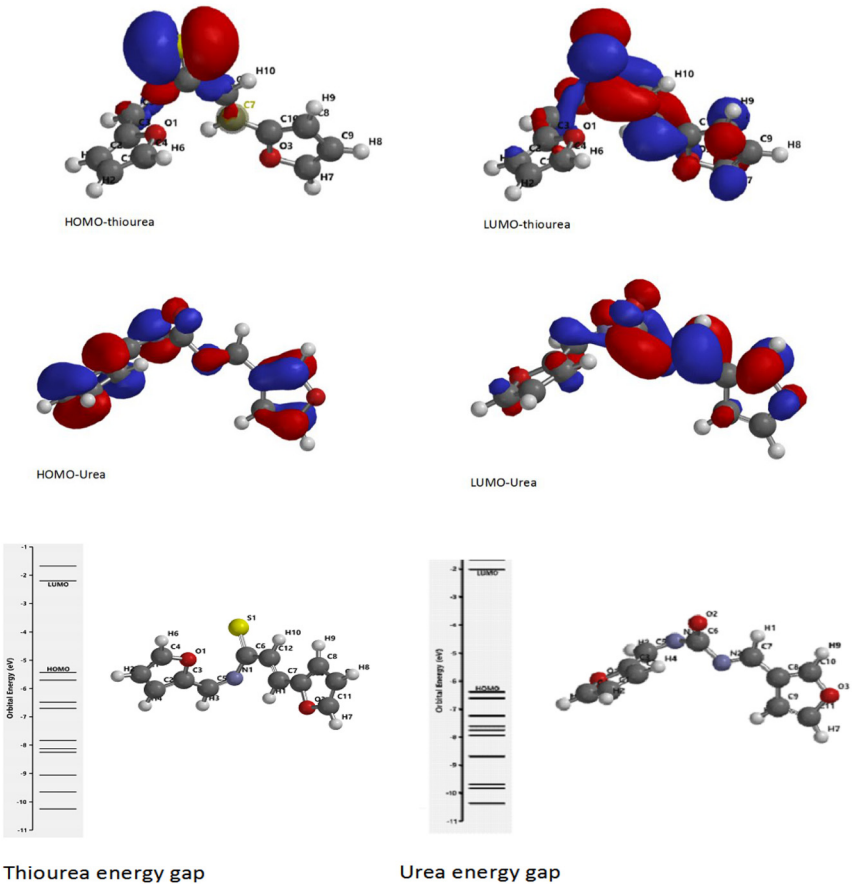

Figure 1: Molecular orbital diagrams and energy gap of BFMT and BFMU.

3 Results and discussion

3.1 Results

3.1.1 Synthesis and percentage yield

3.1.1.1 1,3-Bis[(*E*)-furan-2-yl)methylene]urea

Yield: 92 %, m. p.: 176 °C, MF: $C_{11}H_8N_2O_3$; Elemental analysis: Calcd. (%): C, 61.11; H, 3.73; N, 12.96; O, 22.20; Found (%): C, 61.00; H, 3.84; N, 12.80; O, 22.19; UV: (λ_{max} nm) 348, 390 and 485, IR: (KBr, cm^{-1}) C–H 3155, C=N 1595, C=O 1641, C–O 1228, C–N 1008, C=C 1539, ^{1}H NMR: (6410.3 Hz, DMSO) δ (H, C=C) 2.5 ppm (H, C=C–O) 3.3 ppm (H, –C=N) 6.8 ppm. ^{13}C NMR: (6410.3 Hz, DMSO) δ (C–C, 55 ppm) (C=C–O) 105 and 110 ppm. (C=N) 157.5 ppm (C=O) 160 ppm.

3.1.1.2 1,3-Bis[(*E*)-furan-2-yl)methylene]thiourea

Yield: 70 % m. p.: 190 °C, MF: $C_{11}H_8N_2O_2S$; Elemental analysis: Calcd. (%): C, 56.88; H, 3.47; N, 12.06; O, 13.78; S, 13.81; Found (%): C, 56.90; H, 3.55; N, 12.00; O, 13.77; S, 13.89; UV: (λ_{max} nm) 346, 385 and 485 IR: (KBr, cm^{-1}) C–H 3093-3159 cm^{-1}, C=N 1404 cm^{-1}, C=S 1600 cm^{-1}, C–O 1222 cm^{-1}, C–N 1078 cm^{-1} C=C 1465 cm^{-1} ^{1}H NMR: (6410.3 Hz, DMSO) δ (H, C=C) 2.5 ppm (H, C=C–O) 3.3 ppm (H, –C=N) 7.00 ppm. ^{13}C NMR: (6410.3 Hz, DMSO) δ (C–C, 55 ppm) (C=C–O) 105 and 110 ppm. (C=N) 157.5 ppm (C=S) 170 ppm.

3.1.2 Antimicrobial activities investigated in the samples

3.1.2.1 Antibacterial property

Presented in Table 1 are the results of the zones of inhibition (in mm) incubated at 24 h. BFMU inhibited *P. aeruginosa* and *S. bovis* better than BFMT, while BFMT was better than BFMU in inhibiting *S. typhi*, *S. aureus* and *X. axonopodis*. Compared with Streptomycine sulfate, a standard antibiotic, the two samples were relatively potent.

3.1.3 Antifungal property

The results of antifungal activity of BFMU and BFMT were presented in Table 2. BFMT inhibited the three isolates relatively better than BFMU. Against *F. oxypsorum*, BFMT had 57% while BFMU had 43%, *C. gloeosporioides* was inhibited at 77 and 85% by BFMU and BFMT, respectively. Also BFMT inhibited *C. zeae-maydis* by 60% while BFMU inhibited same at 20%. BFMT values obtained for BFMT were closer to the standard (Mancozeb) used (Table 2).

Table 1: Zones of inhibition (mm) at 24 h incubation.

Samples	*S. typhi*	*S. aureus*	*P. aeruginosa*	*X. axonopodis*	*S. bovis*
BFMU	2.00	3.00	5.00	3.00	4.80
BFMT	4.00	4.00	4.00	4.00	4.00
STREP*	17.00	18.00	14.00	28.00	15.00

*STREP-Streptomycine sulfate (Standard).

Table 2: Antifungal activity of the samples (%) at 72 h of incubation.

Samples	*Fusarium oxysporum*	*Colletotrichum gloeosporioides*	*Cercospora Zeae-maydis*
BFMU	43.07	77.27	20.38
BFMT	57.00	85.71	60.00
*Mancozeb	60.00	90.00	82.00

*Mancozeb is a commercial antifungal used as a control.

3.1.4 Computational results

The investigation of the frontier molecular orbital (FMO) energy levels of the titled compounds indicated that the corresponding electronic transfers happened between the highest occupied molecular orbital (HOMO) and the lowest unoccupied molecular orbital (LUMO). Figure 1 shows the distribution and energy levels of the HOMO and LUMO orbitals computed at the B3LYP/6-31G (d) level for the studied compounds. As observed from Figure 1, in BFMT, the HOMO electrons are mainly delocalized on the azomethine and thiourea fragments while in the LUMO, the electrons are delocalized virtually over all the molecules but less concentrated on one of the furan moieties. However, in the HOMO and LUMO of BFMU, the electrons are delocalized on the whole structure, but more localized on the HOMO of the furan moiety. Molecular orbital coefficient analyses based on B3LYP76-31G (d) optimized geometry indicated that, for the titled compounds, the FMOs are mainly composed of p-atomic orbitals, electronic transitions in the FMOs are derived from the contribution of $n \rightarrow \pi^{\star}$ and $\pi \rightarrow \pi^{\star}$.

The HOMO and LUMO structure analyses further predicted that the sites of activities for the studied compounds are the azomethine and thiourea fragments [11].

The BFMT values for chemical potential, softness, electron affinity and polarizability were 0.52 eV, 0.07 eV, 0.26 eV and 1.06 $\mathring{A}^3$, respectively, higher than that of BFMU (Table 3). It has been reported that the higher the values of these parameters for a substance, the more active the substance. Electron affinity (EA) has direct relationship with the softness of a molecule, thus when the EA is large and positive the molecule should be soft, therefore soft molecules are often more chemically reactive (chemical potential) than hard molecules [18].

In the contrary, BFMU has higher values for the energy gap (see Table 3 and Figure 1), hardness, electrophilicity, electronegativity and ionization energy (Table 3).

Table 3: Global reactivity descriptors of BFMU and BFMT.

Properties	Formulas	BFMU	BFMT	Difference
Energy gap (eV)	$E_L - E_H$	4.54	3.50	1.04
Chemical potential (K)	$\frac{1}{2}(E_H - E_L)$	−2.27	−1.75	−0.52
Hardness (η)	$\frac{1}{2}(E_L - E_H)$	2.27	1.75	0.52
Softness (S)	$\frac{1}{2\eta}$	0.22	0.29	0.07
Electrophilicity (ω)	$\frac{K^2}{2\eta}$	5.85	2.68	3.17
Electronegativity	$\frac{I+EA}{2}$	7.71	4.12	3.59
Ionization potential, I (eV)	$-E_H$	6.65	5.87	0.78
Electron affinity, EA (eV)	$-E_L$	2.11	2.37	0.26
Dipole moment, μ (D)		3.41	3.34	
Polarizability ($\mathring{A}^3$)		57.59	58.65	1.06
E_{HOMO} (eV)		−6.65ev	−5.87ev	
E_{LUMO} (eV)		−2.11ev	−2.37ev	

High ionization energy and energy gap of the BFMU bring about its hardness, indicating the high rigidity or stability and therefore it is less potent. The E_{HOMO} and E_{LUMO} energy gaps (Figure 1) are important stability indices [19]. A large HOMO–LUMO gap of this product also implies high stability for the molecule in chemical reactions [20]. A hard molecule has a large energy gap and a soft molecule has a small energy gap [21]. The electronegativity and hardness are of course used extensively to make predictions about chemical behavior and these are used to explain aromaticity in organic compounds [22].

Also, the electrophilicity index measures the propensity of a species to accept electrons [23, 24]. For the BFMU, the electronegativity and electrophilicity were very high compared with BFMT with differences of 3.59 and 3.17 eV, respectively. This also suggests its low potency.

4 Conclusion

he syntheses of the two compounds were confirmed by spectrometry analyses while their potentialities were confirmed by both experimental and theoretical methods. The results of the two methods agreed with each other. BFMT is a better potential inhibitor of microbes than BFMU, although both could be used as antimicrobial agents especially if the concentration is high. The higher activity shown by BFMT is as a result of the presence of sulfur (S) as its heteroatom. Although in the same group with oxygen (group 6), its ionization energy is lower due to large ionic size and consequently higher activities.

Author contribution: All the authors have accepted responsibility for the entire content of this submitted manuscript and approved submission.
Research funding: None declared.
Conflict of interest statement: The authors declare no conflicts of interest regarding this article.

References

1. Chheda JN, Huber GW, Dumesic JA. Liquid-phase catalytic processing of biomass-derived oxygenated hydrocarbons to fuels and chemicals. Angew Chem Int 2007 [cited 2020];46:7164–83.
2. Zhu YL, Xiang HW, Lil YW, Jiao H, Wu GS, Zhong B, et al. A new strategy for the efficient synthesis of 2-methylfuran and γ-butyrolactone. New J Chem 2003 [cited 2004];27:208–10.
3. Anastas PT, Zimmerman JB. Design through the 12 principles of green engineering. Environ Sci Technol 2003 [cited 1 Mar 2003];37:94A–101A.
4. Moreau RA, Johnston DB, Dickey LC, Parris N, Hicks KB. Aqueous enzymatic oil extraction: a 'green' bioprocess to obtain oil from corn germ and other oil-rich plant materials. ACS Publications; 2007.
5. Moreu RA, Whitaker BD, Hicks KB. Phytosterols, phytostanols, and their conjugates in foods: structural diversity, quantitative analysis, and health-promoting uses. Prog Lipid Res 2002 [cited 2004];41:457–500.

6. Dias AS, Lima S, Carriazo D, Rives V, Pillinger M, Valente AA. Exfoliated titanate, niobate and titanoniobatenanosheets as solid acid catalysts for the liquid-phase dehydration of D-xylose into furfural. J Catal 2006 [cited 2020 June 15];244:230–7.
7. Lime S, Pillinger M, Valente AA. Dehydration of D-xylose into furfural catalysed by solid acids derived from the layered zeolite Nu-6(1). Catal Commun 2008 [cited 2015 April 17];9:2144–8.
8. Lessard J, Morin JF, Wehrung JF, Magnin D, Chornet E. High yield conversion of residual pentoses into furfural via zeolite catalysis and catalytic hydrogenation of furfural to 2-methylfuran. Top Catal 2010 [cited 2014 July 9];53:1231–4.
9. Gomes MG. Síntese de poliésteresa partir do ácido 2,5-Furanodi-carboxílico. M.Sc. Thesis. Portugal: Aveiro University; 2009, vol 12:153–5.pp.
10. Raman JK, Gnansounou E. Furfural production from empty fruit bunch. A Bioref App Ind Crops Prod 2015 [cited 2016];69:371–7.
11. Sonnekar V, Jadhav W, Dake S, Pawar R. Synthesis, antimicrobial and antifungal activities of novel bisimine derivatives. J Phar Bio Chem Sci 2013 [cited 2019 Mar 10];4:1411–8.
12. Adnan D. Synthesis of imine compounds derived from acetylace-tone and structure study. Int J Chem Tech Res 2013 [cited 2018];5:197–203.
13. Jarrahpour AA, Motamedifar M, Pakshir K, Hadi N, Zarei M Pure Chemical Compounds. Moscow: Khimia; 2004 [cited 2017], vol 9:815–24 pp.
14. Coldham I, Dobsona BC, Franklina AI, Fletcherb SR. Synthesis of tetracyclic indole-containing ring systems by intermolecular cycloadditions of azomethine ylides. Tetrahedron Lett 2007 [cited 2019];48:873–5.
15. Alabi KA, Lajide L. Characterization and biological activities of fatty acid amides synthesized from four underutilized plant seed oils. J Chem Pharmaceut Res 2017;9:18–23.
16. Alabi KA, Jabar JM. Sodium tert butoxide: a suitable catalyst for the synthesis of 2-(2-nitrovinyl) furan. FUNAI J Sci Technol 2017;3:85–9.
17. Anbarasan PM, Kumar PS, Geetha M, Govindan R, Manimegalai S, Velmurugan K. Geometries, electronic structures and electronic absorption spectra of silicon dichloride substituted phthalocyanine for dye sensitized solar cells. Recent Res Sci Technol 2010 [cited 2016 Dec 21];2: 8–16.
18. Semire B. Density Functional Theory studies on electronic properties of thiophene S-oxides as aromatic dienophiles for reactivity prediction in Diels-Alder reactions. Pak J Sci Ind Res 2013;56: 14–8.
19. Padmaja L, Ravikumar C, Sajan D, Hubert IJ, Javakumar VS, Pettit GR, et al. Density functional study on the structural conformations and intramolecular charge transfer from the vibrational spectra of the anticancer drug combretastatin-A2. J Raman Spectrosc 2009 [cited 2013];24:401–8.
20. Brian HM, Daniel ER, Alberto S, Marco BN. CO adsorption on noble metal clusters: local environment effects. J Phys Chem C 2011 [cited 2011];115:5637–47.
21. Abdelkader Z, Belkheir H, Ali D, Mohammed B, Hassan Z, Said B, et al. A theoretical study on the inhibition efficiencies of some quinoxalines as corrosion inhibitors of copper in nitric acid. J Saudi Chem Soc 2014 [cited 2015];18:450–5.
22. De Proft F, Geerlings P. Conceptual and computational DFT in the study of aromaticity. Chem Rev 2001 [2001 Apr 24];101:1451–64.
23. Chattaraj PK, Maiti B, Sarkar U. Philicity: a unified treatment of chemical reactivity and selectivity. J Phys Chem 2003 [2006 Feb 4];107:4973–5.
24. Semire B, Odunola OA. Theoretical Study on nucleophilic behaviour of 3,4-Dioxa-7-thia-cylopenta [a]pentalene and 3,7-Dioxa-4-thia-cyclopenta[a]pentalene using ab initio and DFT based reactivity descriptors. Int J Chem Mod 2013 [2016 July 16];4:87–96.